ISSN 1063-7761, Journal of Experimental and Theoretical Physics, 2017, Vol. 125, No. 1, pp. 91–103. © Pleiades Publishing, Inc., 2017.
Original Russian Text © V.A. Ignatchenko, D.S. Polukhin, 2017, published in Zhurnal Eksperimental'noi i Teoreticheskoi Fiziki, 2017, Vol. 152, No. 1, pp. 110–124.

SOLIDS AND LIQUIDS

Development of the Self-Consistent Approximation and Its Application to the Problem of Magnetoelastic Resonance in an Inhomogeneous Medium

V. A. Ignatchenko* and D. S. Polukhin

Kirensky Institute of Physics, Federal Research Center KSC, Siberian Branch, Russian Academy of Sciences, Krasnoyarsk, 660036 Russia

** e-mail: vignatch@iph.krasn.ru*

Received December 22, 2016

Abstract—Our previously proposed approximation involving both the first and second terms of the expansion of the vertex function is generalized to the system of two interacting wavefields of different physical nature. A system of self-consistent equations for the matrix Green's function and matrix vertex function is derived. On the basis of this matrix generalization of the new self-consistent approximation, a theory of magnetoelastic resonance is developed for a ferromagnetic model, where the magnetoelastic coupling parameter $\varepsilon(\mathbf{x})$ is inhomogeneous. Equations for magnetoelastic resonance are analyzed for one-dimensional inhomogeneities of the coupling parameter. The diagonal and off-diagonal elements of the matrix Green's function of the system of coupled spin and elastic waves are calculated with the change in the ratio between the average value ε and rms fluctuation $\Delta\varepsilon$ of the coupling parameter between waves from the homogeneous case ($\varepsilon \neq 0$, $\Delta\varepsilon = 0$) to the extremely randomized case ($\varepsilon = 0$, $\Delta\varepsilon \neq 0$) at various correlation wavenumbers of inhomogeneities k_c. For the limiting case of infinite correlation radius ($k_c = 0$), in addition to approximate expressions, exact analytical expressions corresponding to the summation of all diagrams of elements of the matrix Green's function are obtained. The results calculated for an arbitrary k_c value in the new self-consistent approximation are compared to the results obtained in the standard self-consistent approximation, where only the first term of the expansion of the vertex function is taken into account. It is shown that the new approximation corrects disadvantages of the Green's functions calculated in the standard approximation such as the dome shape of resonances and bends on the sides of resonance peaks. The appearance of a fine structure of the spectrum in the form of a narrow resonance on the Green's function of spin waves and a narrow antiresonance on the Green's function of elastic waves, which was previously predicted in the standard self-consistent approximation, is confirmed. With an increase in the parameter k_c, the Green's functions calculated in the standard and new approximations approach each other and almost coincide with each other at $k_c/k \geq 0.5$. At the same time, the results of this work indicate that the new self-consistent approximation has a certain advantage for studying the problems of stochastic radiophysics in media with long-wavelength inhomogeneities (small k_c values), because it describes both the shape and width of peaks much better than the standard approximation.

DOI: 10.1134/S1063776117060115

1. INTRODUCTION

The self-consistent approximation (SCA), which is widely used in various fields of physics to approximately calculate Green's functions, was introduced by Migdal to study the electron–phonon interaction [1]. A similar variant of the SCA was independently proposed by Kraichnan [2] to study the effect of inhomogeneities on the dynamic susceptibility of waves in disordered media. A similar variant as a generalization of the well-known Born approximation was proposed to study the scattering of electrons in disordered media and was called the self-consistent Born approximation (see, e.g., [3]). We refer to all these variants as the standard SCA. The standard SCA involves only the first term of the expansion of the vertex function and does not involve diagrams with crossing correlation lines (most of the diagrams have these lines). This implies restrictions both on the region of applicability of the standard approximation and on the accuracy of the results. For this reason, corrections to the self-energy caused by the next term in the expansion of the vertex function (vertex corrections) were actively studied [4–13]. A significant progress in studying vertex corrections has been already achieved. However, discrepancy between the results obtained in different approaches is still significant. In [14], we derived a self-consistent approximation of a higher level than that in the standard SCA including both the first and second terms of the series for the vertex function and compared the new and standard SCAs. In [15], we applied the new

SCA to the problem of waves in inhomogeneous media. It is shown that the new self-consistent approximation has a certain advantage for studying the problems of stochastic radiophysics in media with long-wavelength inhomogeneities, because it describes both the shape, width, and height of resonance lines much better than the standard SCA. Consequently, the application of the new SCA to the problem of magnetoelastic resonance in an inhomogeneous medium is of current interest.

The theory of magnetoelastic resonance in the homogeneous medium was developed in fundamental works [16–19], which further stimulated numerous theoretical and experimental studies of this phenomenon. Magnetoelastic resonance is responsible for the appearance of the band gap in the spectrum of spin and elastic waves at the point of intersection of their dispersion curves and, correspondingly, of two resonance peaks on the frequency dependences of the Green's function of the spin and elastic waves. The theory of magnetoelastic resonance in an inhomogeneous medium was developed in [20–23] within the standard SCA. The matrix Green's function of the system of coupled spin and elastic waves was studied at different relations between the average value ε and rms fluctuation $\Delta\varepsilon$ of the coupling parameter between waves from the homogeneous case ($\varepsilon \neq 0$, $\Delta\varepsilon = 0$) to the extremely randomized case ($\varepsilon = 0$, $\Delta\varepsilon \neq 0$). A number of effects have been revealed when resonance peaks approach each other and are joined into one peak with an increase in $\Delta\varepsilon$ and a decrease in ε: a fine structure at the vertices of the Green's functions in the form of a narrow resonance on the Green's function of spin waves and a narrow antiresonance on the Green's function of elastic waves, bends on the sides of peaks, etc. It is of interest to consider how the description of these effects is modified in a more accurate theory of magnetoelastic resonance developed within the new SCA.

The aims of this work are to generalize the new SCA proposed in [14] to the system of two interacting wavefields and to develop a more accurate theory of magnetoelastic resonance in an inhomogeneous medium based on this generalization.

2. SYSTEM OF EQUATIONS FOR MATRIX GREEN'S FUNCTIONS

We consider the model of a ferromagnet where only the dimensionless magnetoelastic coupling parameter $\varepsilon(\mathbf{x})$, $\mathbf{x} = \{x, y, z\}$, is inhomogeneous. Equations of motion for this medium is the Landau–Lifshitz equation for the magnetization vector $\mathbf{M}$ and the equation of motion of elasticity theory for the elastic displacement vector $\mathbf{u}$:

$$\dot{\mathbf{M}} = -g[\mathbf{M}\times\mathbf{H}^e], \tag{1}$$

$$p\ddot{u}_i = \partial\sigma_{ij}/\partial x_j + f_i, \tag{2}$$

where g is the gyromagnetic ratio; p is the density of the medium; σ_{ij} is the stress tensor, where $i, j = x, y, z$; and $\mathbf{f} = \mathbf{f}(\mathbf{x}, t)$ is the external mass force. The effective magnetic field $\mathbf{H}^e$ and stress tensor σ_{ij} have the form

$$\mathbf{H}^e = -\frac{\partial\mathcal{H}}{\partial\mathbf{M}} + \frac{\partial}{\partial\mathbf{x}}\frac{\partial\mathcal{H}}{\partial(\partial\mathbf{M}/\partial\mathbf{x})}, \tag{3}$$

$$\sigma_{ij} = \frac{\partial\mathcal{H}}{\partial u_{ij}}, \tag{4}$$

where $u_{ij} = (\partial u_i/\partial x_j + \partial u_j/\partial x_i)/2$ is the elastic strain tensor. The energy density $\mathcal{H}$ is represented in the form

$$\mathcal{H} = \alpha(\partial\mathbf{M}/\partial x)^2/2 - \mathbf{M}\cdot\mathbf{H} + \lambda u_{ii}^2/2 + \mu u_{ij}^2 + \varepsilon(\mathbf{x})M_iM_ju_{ij}, \tag{5}$$

where α is the exchange parameter, λ and μ are the elastic force constants, $\mathbf{H} = H_0\mathbf{z} + h$, H_0 is the external d.c. magnetic field along the z axis, and $\mathbf{h}$ is the external a.c. magnetic field perpendicular to the z axis. We represent the magnetoelastic parameter $\varepsilon(\mathbf{x})$ in the form

$$\varepsilon(\mathbf{x}) = \varepsilon + \Delta\varepsilon\rho(\mathbf{x}), \tag{6}$$

where ε is the average value of this parameter, $\Delta\varepsilon$ is its rms fluctuation, and $\rho(\mathbf{x})$ is a centered ($\langle\rho(\mathbf{x})\rangle = 0$) and normalized ($\langle\rho^2(\mathbf{x})\rangle = 1$) random function of coordinates. Angle brackets mean the average over the ensemble of realizations of this random function.

The stochastic properties of $\rho(\mathbf{x})$ are characterized by a correlation function depending on the difference of coordinates $\mathbf{r} = \mathbf{x} - \mathbf{x}'$,

$$K(\mathbf{r}) = \langle\rho(\mathbf{x})\rho(\mathbf{x}+\mathbf{r})\rangle \tag{7}$$

or by its Fourier transform, i.e., the spectral density of inhomogeneities

$$S(\mathbf{k}) = \int K(\mathbf{r})e^{-i\mathbf{k}\cdot\mathbf{r}}d\mathbf{r}. \tag{8}$$

Substituting the energy density (5) into equations of motion (1) and (2), we obtain a coupled system of equations for the magnetization $\mathbf{M}$ and displacement $\mathbf{u}$ vectors:

$$-\frac{\dot{\mathbf{M}}}{g} = \left[\mathbf{M}\times\left\{\alpha\Delta\mathbf{M} + \mathbf{H} - \varepsilon(\mathbf{x})M_j\left(\frac{\partial\mathbf{u}}{\partial x_j} + \frac{\partial u_j}{\partial\mathbf{x}}\right)\right\}\right], \tag{9}$$

$$\ddot{\mathbf{u}} = v_t^2\Delta\mathbf{u} + (v_1^2 - v_t^2)\mathrm{graddiv}\mathbf{u} + \frac{1}{p}\frac{\partial}{\partial x_j}(\varepsilon(\mathbf{x})M_j\mathbf{M}) + \frac{\mathbf{f}}{p}, \tag{10}$$

where $v_1 = [(\lambda + 2\mu)/p]^{1/2}$ and $v_t = [\mu/p]^{1/2}$ are the longitudinal and transverse velocities of elastic waves, respectively.

The Landau–Lifshitz equation (9) is linearized by a usual method ($M_z \approx M$; M_x, $M_y \ll M$). For elastic waves, we consider only a model problem: in addition to the condition $v_1 = v_t = v_u$, we impose the condition

$u_z = 0$. Assuming that $M_x, M_y \propto \exp(i\omega t)$ and introducing the circular projections

$$m^{\pm} = M_x \pm iM_y, \quad h^{\pm} = h_x \pm ih_y, \\ u^{\pm} = u_x \pm iu_y, \quad f^{\pm} = f_x \pm if_y, \tag{11}$$

we obtain the following system of two coupled scalar equations for the resonance projections m^+ and u^+ (here and below, the + superscript is omitted):

$$\alpha(\nabla^2 + \nu_m)m - \varepsilon M\frac{\partial u}{\partial z} - (\Delta\varepsilon)M\rho(\mathbf{x})\frac{\partial u}{\partial z} = -h, \tag{12}$$

$$\mu(\nabla^2 + \nu_u)u + \varepsilon M\frac{\partial m}{\partial z} + (\Delta\varepsilon)M\frac{\partial}{\partial z}(\rho(\mathbf{x})m) = -f. \tag{13}$$

Here,

$$\nu_m = \frac{\omega - \omega_0}{\alpha g M}, \quad \nu_u = \frac{\omega^2}{v_u^2}, \tag{14}$$

where ω_0 is the frequency of the homogeneous ferromagnetic resonance, which depends on the magnetic field and demagnetizing factors of the sample and $v_u = \sqrt{\mu/p}$ is the velocity of an elastic wave.

The system of Eqs. (12) and (13) can be represented in the matrix form

$$\{\hat{L}(\mathbf{x}) - \hat{R}(\mathbf{x})\}\hat{Z}(\mathbf{x}) = \hat{F}(\mathbf{x}), \tag{15}$$

where

$$\hat{L}(\mathbf{x}) = \begin{bmatrix} \nabla^2 + \nu_m & -\dfrac{\varepsilon M}{\mu}\dfrac{\partial}{\partial z} \\ \dfrac{\varepsilon M}{\alpha}\dfrac{\partial}{\partial z} & \nabla^2 + \nu_u \end{bmatrix}, \tag{16}$$

$$\hat{R}(\mathbf{x}) = \begin{bmatrix} 0 & \dfrac{\Delta\varepsilon}{\mu}M\rho(\mathbf{x})\dfrac{\partial}{\partial z} \\ -\dfrac{\Delta\varepsilon}{\mu}M\left(\dfrac{\partial}{\partial z}\rho(\mathbf{x}) + \rho(\mathbf{x})\dfrac{\partial}{\partial z}\right) & 0 \end{bmatrix}, \tag{17}$$

$$\hat{Z}(\mathbf{x}) = \begin{bmatrix} \alpha m \\ \mu u \end{bmatrix}, \quad \hat{F}(\mathbf{x}) = \begin{bmatrix} -h \\ -f \end{bmatrix}. \tag{18}$$

According to this representation, αm and μu are the normalized variables for the coupled system of equations. We also use this normalization to introduce the matrix Green's function and to write the equation for it in the form

$$[\hat{L}(\mathbf{x}) - \hat{R}(\mathbf{x})]\hat{\tilde{G}}(\mathbf{x}, \mathbf{x}_0) = \delta(\mathbf{x} - \mathbf{x}_0)\hat{E}. \tag{19}$$

Here,

$$\hat{\tilde{G}}(\mathbf{x}, \mathbf{x}_0) = \begin{bmatrix} \tilde{G}_{mm}(\mathbf{x}, \mathbf{x}_0) & \tilde{G}_{mu}(\mathbf{x}, \mathbf{x}_0) \\ \tilde{G}_{um}(\mathbf{x}, \mathbf{x}_0) & \tilde{G}_{uu}(\mathbf{x}, \mathbf{x}_0) \end{bmatrix}, \tag{20}$$

where $\tilde{G}_{mm}$ and $\tilde{G}_{mu}$ are the spin Green's functions at the magnetic and elastic point excitations, respectively; $\tilde{G}_{uu}$ and $\tilde{G}_{um}$ are the elastic Green's function at the elastic and magnetic point excitations, respectively; and

$$\hat{E} = \begin{bmatrix} 1 & 0 \\ 0 & 1 \end{bmatrix} \tag{21}$$

is the identity matrix.

We represent the Green's function $\hat{\tilde{G}}$ in the form

$$\hat{\tilde{G}} = \hat{g} + \hat{\tilde{G}}', \tag{22}$$

where $\hat{g}$ is the initial Green's function and $\hat{\tilde{G}}'$ is the correction caused by the inhomogeneous part of the coupling parameter.

The substitution of Eq. (22) into Eq. (19) gives the following equation for $\hat{g}$ and $\hat{\tilde{G}}'$:

$$\hat{L}(\mathbf{x})\hat{g}(\mathbf{x}, \mathbf{x}_0) = \delta(\mathbf{x} - \mathbf{x}_0)\hat{E}, \tag{23}$$

$$\hat{L}(\mathbf{x})\hat{\tilde{G}}'(\mathbf{x}, \mathbf{x}_0) = \hat{R}(\mathbf{x})\hat{\tilde{G}}(\mathbf{x} - \mathbf{x}_0). \tag{24}$$

Equation (23) for the initial Green's function $\hat{g}(\mathbf{x}, \mathbf{x}_0)$, which describes coupled magnetoelastic waves in a homogeneous medium, can be solved exactly. We now analyze Eq. (24) for the correction $\hat{\tilde{G}}'(\mathbf{x}, \mathbf{x}_0)$. According to the general rules, a formal solution of Eq. (24) can be represented in the form of an integral of the product of the unperturbed Green's function and the right-hand side of this equation. Substituting this solution into Eq. (22), we obtain the following generating integral equation for the matrix Green's function $\hat{\tilde{G}}'$

$$\hat{\tilde{G}}(\mathbf{x}, \mathbf{x}_0) = \tilde{g}(\mathbf{x}, \mathbf{x}_0) \\ + \int \hat{\tilde{G}}(\mathbf{x}, \mathbf{x}')\hat{R}(\mathbf{x}')\hat{g}(\mathbf{x}', \mathbf{x}_0)d\mathbf{x}'. \tag{25}$$

Here, we transpose the functions $\hat{g}$ and $\hat{\tilde{G}}$ in the integrand; the necessity of such transposition was justified in [14]. The elements of the matrix $\hat{R}$ include derivatives of the random function $\rho(\mathbf{x})$, which is inconvenient for the subsequent use. For this reason, we transform the integral in Eq. (25) by integration by parts for each element of the matrix, as was made in [21]. Extracting γ and ρ from the matrix $\hat{R}$, we obtain a generating integral equation for the matrix Green's function $\hat{\tilde{G}}$ in the form

$$\hat{\tilde{G}}(\mathbf{x}, \mathbf{x}_0) = \hat{g}(\mathbf{x}, \mathbf{x}_0) \\ + \gamma \int \rho(\mathbf{x}')\hat{Y}(\mathbf{x}, \mathbf{x}')\hat{J}\hat{Y}_0(\mathbf{x}', \mathbf{x}_0)d\mathbf{x}', \tag{26}$$

where

$$\hat{Y}(\mathbf{x}, \mathbf{x}') = \begin{bmatrix} \tilde{G}_{mm}(\mathbf{x}, \mathbf{x}') & \dfrac{\partial \tilde{G}_{mu}(\mathbf{x}, \mathbf{x}')}{\partial z'} \\ \tilde{G}_{um}(\mathbf{x}, \mathbf{x}') & \dfrac{\partial \tilde{G}_{uu}(\mathbf{x}, \mathbf{x}')}{\partial z'} \end{bmatrix}, \tag{27}$$

$$\hat{Y}_0(\mathbf{x}',\mathbf{x}_0)=\begin{bmatrix} g_{mm}(\mathbf{x}',\mathbf{x}_0) & g_{mu}(\mathbf{x}',\mathbf{x}_0) \\ \dfrac{\partial g_{um}(\mathbf{x}',\mathbf{x}_0)}{\partial z'} & \dfrac{\partial g_{uu}(\mathbf{x}',\mathbf{x}_0)}{\partial z'} \end{bmatrix}, \tag{28}$$

$$\hat{J}=\begin{bmatrix} 0 & \sqrt{\alpha/\mu} \\ \sqrt{\mu/\alpha} & 0 \end{bmatrix}, \tag{29}$$

$$\gamma=\frac{\Delta\varepsilon}{\sqrt{\alpha\mu}}M. \tag{30}$$

Rewriting Eqs. (27) and (28) in the form

$$\hat{Y}(\mathbf{x},\mathbf{x}')=\hat{\tilde{G}}(\mathbf{x},\mathbf{x}')\hat{E}_1(\mathbf{x}'), \tag{31}$$

$$\hat{Y}_0(\mathbf{x}',\mathbf{x}_0)=\hat{E}_1(\mathbf{x}')\hat{g}(\mathbf{x}',\mathbf{x}_0), \tag{32}$$

where

$$\hat{E}_1(\mathbf{x}')=\begin{bmatrix} 1 & 0 \\ 0 & \dfrac{\partial}{\partial z'} \end{bmatrix}, \tag{33}$$

we arrive at the generating integral equation for the matrix Green's function $\hat{\tilde{G}}$ in the final form

$$\begin{aligned}\hat{\tilde{G}}(\mathbf{x},\mathbf{x}_0)&=\hat{g}(\mathbf{x},\mathbf{x}_0)+\gamma\int\rho(\mathbf{x}'')\hat{\tilde{G}}(\mathbf{x},\mathbf{x}'')\\ &\times\hat{E}_1(\mathbf{x}'')\hat{J}\hat{E}_1(\mathbf{x}'')\hat{g}(\mathbf{x}'',\mathbf{x}_0)d\mathbf{x}''.\end{aligned} \tag{34}$$

For convenience of below algebra, we change the variable of integration $\mathbf{x}'$ in Eq. (34) to $\mathbf{x}''$. Using the usual procedure of successive iterations of Eq. (34), we obtain a series for the matrix Green's function $\hat{\tilde{G}}$:

$$\begin{aligned}\hat{\tilde{G}}(\mathbf{x},\mathbf{x}_0)&=\hat{g}(\mathbf{x},\mathbf{x}_0)+\gamma\int\rho(\mathbf{x}'')\hat{g}(\mathbf{x},\mathbf{x}'')\\ &\times\hat{E}_1(\mathbf{x}'')\hat{J}\hat{E}_1(\mathbf{x}'')\hat{g}(\mathbf{x}'',\mathbf{x}_0)d\mathbf{x}''+\gamma^2\iint\rho(\mathbf{x}')\rho(\mathbf{x}'')\\ &\times\hat{g}(\mathbf{x},\mathbf{x}')\hat{E}_1(\mathbf{x}')\hat{J}\hat{E}_1(\mathbf{x}')\hat{g}(\mathbf{x}',\mathbf{x}'')\\ &\times\hat{E}_1(\mathbf{x}'')\hat{J}\hat{E}_1(\mathbf{x}'')\hat{g}(\mathbf{x}'',\mathbf{x}_0)d\mathbf{x}'d\mathbf{x}''+\ldots\end{aligned} \tag{35}$$

Averaging this series over the ensemble of realizations of the random function $\rho(\mathbf{x})$ and decoupling the correlation functions by the Gauss formula, we arrive at the series for the averaged matrix Green's function:

$$\begin{aligned}\hat{G}(\mathbf{x},\mathbf{x}_0)&=\hat{g}(\mathbf{x},\mathbf{x}_0)+\gamma^2\iint K(\mathbf{x}',\mathbf{x}'')\hat{g}(\mathbf{x},\mathbf{x}')\\ &\times\hat{E}_1(\mathbf{x}')\hat{J}\hat{E}_1(\mathbf{x}')\hat{g}(\mathbf{x}',\mathbf{x}'')\hat{E}_1(\mathbf{x}'')\\ &\times\hat{J}\hat{E}_1(\mathbf{x}'')\hat{g}(\mathbf{x}'',\mathbf{x}_0)d\mathbf{x}'d\mathbf{x}''+\ldots.\end{aligned} \tag{36}$$

We represent this series in the form of the matrix Dyson equation

$$\begin{aligned}\hat{G}(\mathbf{x},\mathbf{x}_0)&=\hat{g}(\mathbf{x},\mathbf{x}_0)+\iint\hat{G}(\mathbf{x},\mathbf{x}')\hat{E}_1(\mathbf{x}')\\ &\times\hat{\Sigma}(\mathbf{x}',\mathbf{x}'')\hat{E}_1(\mathbf{x}'')\hat{g}(\mathbf{x}'',\mathbf{x}_0)d\mathbf{x}'d\mathbf{x}'',\end{aligned} \tag{37}$$

where the self-energy $\hat{\Sigma}$ has the form

$$\begin{aligned}\hat{\Sigma}(\mathbf{x}',\mathbf{x}'')&=\gamma^2\iint K(\mathbf{x}_2,\mathbf{x}'')\hat{\Gamma}(\mathbf{x}',\mathbf{x}_1;\mathbf{x}_2)\\ &\times\hat{J}\hat{X}(\mathbf{x}_1,\mathbf{x}'')\hat{J}d\mathbf{x}_1d\mathbf{x}_2.\end{aligned} \tag{38}$$

Here, the matrix vertex function is a series in powers of γ^2. Retaining the first two terms of this series, we obtain

$$\begin{aligned}\hat{\Gamma}(\mathbf{x}',\mathbf{x}_1;\mathbf{x}_2)&\approx\delta(\mathbf{x}'-\mathbf{x}_2)\delta(\mathbf{x}'-\mathbf{x}_1)\hat{E}\\ &+\gamma^2\iiiint K(\mathbf{x}_1,\mathbf{x}_4)\hat{\Gamma}(\mathbf{x}',\mathbf{x}_3;\mathbf{x}_4)\hat{J}\hat{X}(\mathbf{x}_3,\mathbf{x}_5)\\ &\times\hat{\Gamma}(\mathbf{x}_5,\mathbf{x}_6;\mathbf{x}_2)\hat{J}\hat{X}(\mathbf{x}_6,\mathbf{x}_1)d\mathbf{x}_3d\mathbf{x}_4d\mathbf{x}_5d\mathbf{x}_6,\end{aligned} \tag{39}$$

where

$$\hat{X}(\mathbf{x}_1,\mathbf{x}'')=\hat{E}_1(\mathbf{x}_1)\hat{G}(\mathbf{x}_1,\mathbf{x}'')\hat{E}_1(\mathbf{x}''). \tag{40}$$

Subscripts of arguments in all vertex functions correspond to similar subscripts in Eq. (21) in [14] because the same generating integral equation (25) corresponding to the transposed functions $\hat{g}$ and $\hat{\tilde{G}}$ is used in both cases. Consequently, the further derivation of the self-consistent approximation for the matrix vertex function (39) is similar to the derivation of the same approximation for the scalar vertex function in [14].

3. SELF-CONSISTENT APPROXIMATION FOR THE MATRIX VERTEX FUNCTION

We take the Fourier transforms of all matrix quantities

$$\hat{Y}(\mathbf{x})=(2\pi)^{-d}\int\hat{Y}_{\mathbf{k}}e^{i\mathbf{k}\cdot\mathbf{x}}d\mathbf{k}, \tag{41}$$

$$\hat{Y}_{\mathbf{k}}=\int\hat{Y}(\mathbf{x})e^{-i\mathbf{k}\cdot\mathbf{x}}d\mathbf{x}, \tag{42}$$

where d is the dimension of the space. Then, substituting the Fourier transform of Eq. (39) into the Fourier transform of Eq. (38), we find an approximate expression for the self-energy $\hat{\Sigma}$ in the $\mathbf{k}$ space. Equating the exact and approximate expressions for the self-energy $\hat{\Sigma}$, we arrive at a matrix analog of the new self-consistent approximation derived for scalar functions in [14]:

$$\begin{aligned}\hat{G}_{\mathbf{k}}&=\hat{E}\Big\{\hat{g}_{\mathbf{k}}^{-1}-\gamma^2(2\pi)^{-d}\hat{E}_{\mathbf{k}}^{(1)}\\ &\times\int S_{\mathbf{k}-\mathbf{k}_1}\hat{J}\hat{X}_{\mathbf{k}_1}\hat{\Gamma}_{\mathbf{k}_1,\mathbf{k}-\mathbf{k}_1}\hat{J}d\mathbf{k}_1\hat{E}_{\mathbf{k}}^{(2)}\Big\}^{-1},\end{aligned} \tag{43}$$

$$\begin{aligned}\hat{\Gamma}_{\mathbf{k}_1,\mathbf{k}-\mathbf{k}_1}&\approx\hat{E}\Big\{\hat{E}-\gamma^2(2\pi)^{-d}\\ &\times\int S_{\mathbf{k}_1-\mathbf{k}_2}\hat{\Gamma}_{\mathbf{k}_2,\mathbf{k}_1-\mathbf{k}_2}\hat{J}\hat{X}_{\mathbf{k}_2}\hat{J}\hat{X}_{\mathbf{k}-\mathbf{k}_1+\mathbf{k}_2}d\mathbf{k}_2\Big\}^{-1}.\end{aligned} \tag{44}$$

Here,

$$\hat{X}_{\mathbf{k}_1}=\hat{E}_{\mathbf{k}_1}^{(2)}\hat{G}_{\mathbf{k}_1}\hat{E}_{\mathbf{k}_1}^{(1)}, \tag{45}$$

$$\begin{aligned}\hat{g}_{\mathbf{k}}^{-1}&=\begin{bmatrix} \nu_m-k^2 & -i(\varepsilon/\mu)Mk_z \\ i(\varepsilon/\alpha)Mk_z & \nu_u-k^2 \end{bmatrix},\\ \hat{g}_{\mathbf{k}}&=\begin{bmatrix} g_{mm}(\mathbf{k}) & ig_{mu}(\mathbf{k}) \\ -ig_{um}(\mathbf{k}) & g_{uu}(\mathbf{k}) \end{bmatrix},\end{aligned} \tag{46}$$

$$\hat{E}_{\mathbf{k}}^{(1)} = \begin{bmatrix} 1 & 0 \\ 0 & -ik_z \end{bmatrix}, \quad \hat{E}_{\mathbf{k}}^{(2)} = \begin{bmatrix} 1 & 0 \\ 0 & ik_z \end{bmatrix}. \tag{47}$$

We represent the matrix Green's function $\hat{G}_{\mathbf{k}}$ similar to the initial matrix Green's function $\hat{g}_{\mathbf{k}}$ in the form

$$\hat{G}_{\mathbf{k}} = \begin{bmatrix} G_{mm}(\mathbf{k}) & iG_{mu}(\mathbf{k}) \\ -iG_{um}(\mathbf{k}) & G_{uu}(\mathbf{k}) \end{bmatrix}. \tag{48}$$

The components of the initial matrix Green's function $\hat{g}_{\mathbf{k}}$ have the form

$$\begin{aligned} g_{mm}(\mathbf{k}) &= \frac{\nu_u - k^2}{(\nu_m - k^2)(\nu_u - k^2) - \gamma_0^2 k_z^2}, \\ g_{mu}(\mathbf{k}) &= \frac{(\varepsilon/\mu)Mk_z}{(\nu_m - k^2)(\nu_u - k^2) - \gamma_0^2 k_z^2}, \\ g_{um}(\mathbf{k}) &= \frac{(\varepsilon/\alpha)Mk_z}{(\nu_m - k^2)(\nu_u - k^2) - \gamma_0^2 k_z^2}, \\ g_{uu}(\mathbf{k}) &= \frac{\nu_m - k^2}{(\nu_m - k^2)(\nu_u - k^2) - \gamma_0^2 k_z^2}, \end{aligned} \tag{49}$$

where

$$\gamma_0 = \frac{\varepsilon}{\sqrt{\alpha\mu}} M. \tag{50}$$

Each term in the expansion of the vertex function (44) in series in γ^2 includes the repeated products of the matrices $\hat{J}\hat{X}$. The same repetition of matrix products is obtained for the desired Green's function (43) by multiple substitution of the resulting branched continued fraction into Eqs. (43) and (44) and expanding in a series in γ^2. For example, we present one term of the series with crossing correlation lines, which is proportional to γ^4:

$$\begin{aligned} &\gamma^4 (2\pi)^{-2d} \hat{X}_{\mathbf{k}}^{(0)} \iint S_{\mathbf{k}-\mathbf{k}_1} S_{\mathbf{k}_1-\mathbf{k}_2} \\ &\times \hat{J}\hat{X}_{\mathbf{k}_1}^{(0)} \hat{J}\hat{X}_{\mathbf{k}_2}^{(0)} \hat{J}\hat{X}_{\mathbf{k}-\mathbf{k}_1+\mathbf{k}_2}^{(0)} \hat{J}\hat{X}_{\mathbf{k}}^{(0)} d\mathbf{k}_1 d\mathbf{k}_2. \end{aligned} \tag{51}$$

The product of $\hat{J}\hat{X}_{\mathbf{k}_1}^{(0)}\hat{J}$ and $\hat{J}\hat{X}_{\mathbf{k}-\mathbf{k}_1+\mathbf{k}_2}^{(0)}\hat{J}$, where $\hat{X}_{\mathbf{k}_1}^{(0)} = \hat{E}_{\mathbf{k}_1}^{(2)} \hat{g}_{\mathbf{k}_1} \hat{E}_{\mathbf{k}_1}^{(1)}$, gives matrices whose elements are transposed with respect to $\hat{X}^{(0)}$, e.g.:

$$\hat{X}_{\mathbf{k}_1}^{(0)} = \begin{bmatrix} g_{mm}(\mathbf{k}_1) & k_{1z} g_{mu}(\mathbf{k}_1) \\ k_{1z} g_{um}(\mathbf{k}_1) & k_{1z}^2 g_{uu}(\mathbf{k}_1) \end{bmatrix}, \tag{52}$$

$$\begin{aligned} \hat{\tilde{X}}_{\mathbf{k}_1}^{(0)} &= \hat{J}\hat{X}_{\mathbf{k}_1}^{(0)}\hat{J} \\ &= \begin{bmatrix} k_{1z}^2 g_{uu}(\mathbf{k}_1) & (\alpha/\mu) k_{1z} g_{um}(\mathbf{k}_1) \\ (\mu/\alpha) k_{1z} g_{mu}(\mathbf{k}_1) & g_{mm}(\mathbf{k}_1) \end{bmatrix} \end{aligned} \tag{53}$$

Thus removing off-diagonal matrices $\hat{J}$, we obtain

$$\begin{aligned} &\gamma^4 (2\pi)^{-2d} \hat{X}_{\mathbf{k}}^{(0)} \iint S_{\mathbf{k}-\mathbf{k}_1} S_{\mathbf{k}_1-\mathbf{k}_2} \\ &\times \hat{\tilde{X}}_{\mathbf{k}_1}^{(0)} \hat{X}_{\mathbf{k}_2}^{(0)} \hat{\tilde{X}}_{\mathbf{k}-\mathbf{k}_1+\mathbf{k}_2}^{(0)} \hat{X}_{\mathbf{k}}^{(0)} d\mathbf{k}_1 d\mathbf{k}_2. \end{aligned} \tag{54}$$

Alternation of matrices $\hat{\tilde{X}}$ and $\hat{X}$ is characteristic of all terms of the series because the interaction is transferred from a spin wave to an elastic wave, from the elastic wave to the spin wave, etc.

The matrix analog of the new self-consistent approximation given by Eqs. (43) and (44) contains all matrix analogs of lower-level approximations. Neglecting the term of the order γ^2 in the denominator of Eq. (44), we obtain $\hat{\Gamma}_{k_1,k-k_1}^{(m)} = \hat{E}$. The substitution of this expression into Eq. (43) gives a matrix analog of the standard SCA:

$$\begin{aligned} \hat{G}_{\mathbf{k}} &= \hat{E}\Big\{\hat{g}_{\mathbf{k}}^{-1} - \gamma^2 (2\pi)^{-d} \hat{E}_{\mathbf{k}}^{(1)} \\ &\times \int S_{\mathbf{k}-\mathbf{k}_1} \hat{J}\hat{E}_{\mathbf{k}_1}^{(2)} \hat{G}_{\mathbf{k}_1} \hat{E}_{\mathbf{k}_1}^{(1)} \hat{J} d\mathbf{k}_1 \hat{E}_{\mathbf{k}}^{(2)} \Big\}^{-1}. \end{aligned} \tag{55}$$

The first iteration of Eq. (55), $\hat{G}_{\mathbf{k}_1} = \hat{g}_{\mathbf{k}_1}$, provides a matrix analog of the non-self-consistent Bourret (Born) approximation [3, 24, 25]:

$$\begin{aligned} \hat{G}_{\mathbf{k}} &= \hat{E}\Big\{\hat{g}_{\mathbf{k}}^{-1} - \gamma^2 (2\pi)^{-d} \hat{E}_{\mathbf{k}}^{(1)} \\ &\times \int S_{\mathbf{k}-\mathbf{k}_1} \hat{J}\hat{E}_{\mathbf{k}_1}^{(2)} \hat{g}_{\mathbf{k}_1} \hat{E}_{\mathbf{k}_1}^{(1)} \hat{J} d\mathbf{k}_1 \hat{E}_{\mathbf{k}}^{(2)} \Big\}^{-1}. \end{aligned} \tag{56}$$

4. ANALYSIS OF ELEMENTS OF THE MATRIX GREEN'S FUNCTION

Below, we consider only one-dimensional inhomogeneities of the coupling parameter $\varepsilon(\mathbf{x}) = \varepsilon(z)$. Then, in all equations (43)–(54), $d = 1$ and the vector $\mathbf{k}$ has the single component $k_z = k$. The correlation properties of the random function $\rho(x)$ are simulated by an exponential correlation function

$$K(r) = e^{-k_c|x-x'|}, \quad S_k = \frac{2k_c}{k_c^2 + k^2}, \tag{57}$$

where $r = |x - x'|$ and k_c is the correlation wavenumber ($r_c = k_c^{-1}$ is the correlation radius of inhomogeneities).

For the numerical analysis, we write the system of equations (43) and (44) in the form of recurrence formulas:

$$\begin{aligned} \hat{G}_k^{(n)} &= \hat{E}\Big\{\hat{g}_k^{-1} - \gamma^2 (2\pi)^{-1} \hat{E}_k^{(1)} \int S_{k-k_1} \\ &\times \hat{J}\hat{E}_{k_1}^{(2)} \hat{G}_{k_1}^{(n-1)} \hat{E}_{k_1}^{(1)} \hat{\Gamma}_{k_1,k-k_1}^{(m)} \hat{J} dk_1 \hat{E}_k^{(2)} \Big\}^{-1}, \end{aligned} \tag{58}$$

$$\begin{aligned} \hat{\Gamma}_{k_1,k-k_1}^{(m)} &\approx \hat{E}\Big\{\hat{E} - \gamma^2 (2\pi)^{-d} \int S_{k_1-k_2} \\ &\times \hat{\Gamma}_{k_2,k_1-k_2}^{(m-1)} \hat{J}\hat{E}_{k_2}^{(2)} \hat{G}_{k_2}^{(n)} \hat{E}_{k_2}^{(1)} \hat{J}\hat{E}_{k-k_1+k_2}^{(2)} \\ &\times \hat{G}_{k-k_1+k_2}^{(n)} \hat{E}_{k-k_1+k_2}^{(1)} dk_2 \Big\}^{-1}, \end{aligned} \tag{59}$$

where the superscripts n and m correspond to the iteration processes for the Green's function and vertex function, respectively.

With the growth of inhomogeneities, ε decreases from its initial value ε_0 to zero, whereas $\Delta\varepsilon$ increases from zero to a certain maximum value ε' close to ε_0. For simplicity, we set $\varepsilon' = \varepsilon_0$ and analyze change in the elements of the Green's functions at the crossing resonance point $k = k_r$ with an increase in $\Delta\varepsilon$ and with a decrease in ε at the conservation of the sum of squares of these quantities, as was proposed in [22]:

$$\varepsilon^2 + (\Delta\varepsilon)^2 = \varepsilon_0^2. \tag{60}$$

Experimental samples, where intermediate states between two limiting cases—homogenous ($\varepsilon = \varepsilon_0$, $\Delta\varepsilon = 0$) and completely randomized ($\varepsilon = 0$, $\Delta\varepsilon = \varepsilon_0$)—are created by varying their composition or the processing method, do not necessarily satisfy Eq. (60). This relation is introduced only for the convenient step-by-step consideration of all intermediate states with different relations between $(\varepsilon/\varepsilon_0)^2$ and $(\Delta\varepsilon/\varepsilon_0)^2$. The gap in the spectrum of magnetoelastic waves appears at the point of intersection of unperturbed dispersion laws ($k = k_r$, $\omega = \omega_r$) with the width Λ proportional to the coupling parameter in a homogeneous medium ε_0

$$\Lambda = \frac{\varepsilon_0 M}{\sqrt{\mu}}\sqrt{2\omega_M\omega_r}, \tag{61}$$

where $\omega_m = gM$. The quantity Λ determines also the distance between two maxima on the frequency dependence of the imaginary part of the Green's function of both spin and elastic waves in the magnetoelastic resonance region in the homogeneous medium. The dimensionless frequency on all plots presented below is given in units of Λ.

We first consider the limiting case of infinite radius of correlations ($k_c = 0$). In this case, the spectral density is represented in terms of a delta function: $S(k - k_1) = 2\pi\delta(k - k_1)$ and the integral terms of continued fractions (58) and (59) become algebraic. This circumstance strongly simplifies the calculations of Green's functions in both new and standard SCAs. Furthermore, in this situation, it is possible to find the exact Green's function (an analog of the Keldysh model [26] for the matrix Green's function). In this case, random functions $\rho(\mathbf{x})$ are transformed to random values whose stochastic properties are described by a certain distribution function $f(\rho)$. The exact Green's function for this situation is calculated by the method that we used to determine the exact scalar Green's function of waves in the inhomogeneous medium [22]. To this end, we return to the initial system of two scalar equations (12) and (13) for resonance projections m^+ and u^+. These equations at $k_c = 0$ become equations with constant coefficients and their analytical solutions are easily obtained after the Fourier transform. Exact analytical solutions of the matrix equation (19) for the unaveraged Green's function of the system are also easily found in the $\mathbf{k}$ space:

$$\breve{\hat{G}}(\omega, k; \rho) = \begin{bmatrix} \breve{G}_{mm}(\omega, k; \rho) & i\breve{G}_{mu}(\omega, k; \rho) \\ -i\breve{G}_{um}(\omega, k; \rho) & \breve{G}_{uu}(\omega, k; \rho) \end{bmatrix}, \tag{62}$$

where

$$\begin{aligned} \breve{G}_{mm}(\omega, k; \rho) &= \frac{\nu_u - k^2}{(\nu_m - k^2)(\nu_u - k^2) - (\gamma_0 + \gamma\rho)^2 k^2}, \\ \breve{G}_{mu}(\omega, k; \rho) &= \frac{\sqrt{\alpha/\mu}k(\gamma_0 + \gamma\rho)}{(\nu_m - k^2)(\nu_u - k^2) - (\gamma_0 + \gamma\rho)^2 k^2}, \\ \breve{G}_{um}(\omega, k; \rho) &= \frac{\sqrt{\mu/\alpha}k(\gamma_0 + \gamma\rho)}{(\nu_m - k^2)(\nu_u - k^2) - (\gamma_0 + \gamma\rho)^2 k^2}, \\ \breve{G}_{uu}(\omega, k; \rho) &= \frac{\nu_m - k^2}{(\nu_m - k^2)(\nu_u - k^2) - (\gamma_0 + \gamma\rho)^2 k^2}. \end{aligned} \tag{63}$$

These expressions differ from Eqs. (49) for the initial matrix Green's function $\hat{g}_{\mathbf{k}}$ only in the presence of random values ρ and at $\gamma = 0$ coincide with Eqs. (49).

The averaged matrix Green's function is given by the expression

$$\hat{\bar{G}}(\omega, k) = \int \hat{\breve{G}}(\omega, k; \rho) f(\rho) d\rho, \tag{64}$$

where $f(\rho)$ is the distribution function of random values ρ, which can generally have an arbitrary form. For the situation considered here, when the decoupling of correlation functions in Eq. (35) is performed by the Gaussian function, $f(\rho)$ is the Gaussian function

$$f(\rho) = \frac{1}{(2\pi)^{1/2}} e^{-\rho^2/2}. \tag{65}$$

Figure 1 shows the imaginary parts $G''_{mm}(\omega)$ of the Green's function of spin waves in the region of magnetoelastic resonance for the case $k_c = 0$ obtained (red dashed curves) in the standard SCA, (black solid lines) in the new SCA, and (blue dotted curves) by the exact summation of all diagrams. The width of peaks that is due to the random distribution of frequencies increases with an increase in the rms fluctuation $\Delta\varepsilon$ and with a decrease in the average value ε of the coupling parameter between spin and elastic waves. Peaks gradually approach each other and, finally, are joined into one wide peak. It is seen that the standard SCA (Eq. (55)) reveals a number of unusual effects: dome shape of resonances, curves with three maxima (Fig. 1b), bends on sides of the peak (Fig. 1c). Similar effects were

observed in [20–23], where the theory of magnetoelastic resonance was developed in the standard SCA. In those works, these effects were attributed to disadvantages of the standard SCA and, to justify this assumption, a simplified model of overlapping of two noninteracting dome-shaped resonances was considered. In the more accurate theory of magnetoelastic resonance developed in this work, all these strange effects are absent on plots of exact Green's functions (Eq. (64)) and on plots of the new SCA corresponding to the system of Eqs. (58) and (59). The new SCA describes both the shape and widths of peaks much better than the standard SCA and gives plots close to the exact curves. Beginning with the ordered case ($\varepsilon \neq 0$, $\Delta\varepsilon = 0$) and ending with the case of the complete randomization of the coupling parameter ($\varepsilon = 0$, $\Delta\varepsilon \neq 0$), two narrow peaks are smoothly transformed to a single wide peak. The imaginary parts $G''_{uu}(\omega)$ of the Green's functions of elastic waves are not presented in Fig. 1 because they differ from the imaginary parts $G''_{mm}(\omega)$ of the Green's function of spin waves only in a larger height of resonance peaks. This follows from the relation obtained for the case $k_c = 0$ in [22],

$$\frac{G_{mm}(\omega, k_r)}{G_{uu}(\omega, k_r)} = \frac{v_m}{v_u}, \qquad (66)$$

where $v_m < v_u$, $v_m = 2\alpha g M k_r$ is the velocity of spin waves in the region of magnetoelastic resonance.

We now consider the general case corresponding to an arbitrary correlation wavenumber of inhomogeneities k_c. Figure 2 shows the imaginary parts $G''_{mm}(\omega)$ and $G''_{uu}(\omega)$ of the diagonal elements of the matrix Green's function of spin and elastic waves, respectively, for the case $\kappa_c = k_c/k_r = 0.01$. It is seen that even such a small κ_c value significantly changes the shape of resonance peaks. First, the shape of resonance peaks of the Green's function of elastic waves $G''_{uu}(\omega)$ now does not coincide with the shape of peaks of the Green's function of spin waves $G''_{mm}(\omega)$. Second, with an increase in $\Delta\varepsilon$, a fine structure of the spectrum appears near $\omega = \omega_r$: a narrow peak (resonance) on the Green's function of spin waves $G''_{mm}(\omega)$ (Fig. 2) and a dip (antiresonance) on the Green's function of elastic waves $G''_{uu}(\omega)$. This fine structure of the spectrum was predicted and studied in our works [20–23], where the theory of magnetoelastic resonance in an inhomogeneous medium was developed in the standard SCA (red dashed curves in Fig. 2). In spite of significant differences in the shape of resonance peaks calculated in the standard and new SCAs, the main properties of the fine structure of the spectrum are revealed in both the new and standard SCAs. In particular, if the plots in the right panels of Fig. 2 (taking into account their scale) are imposed on the respective plots in the left panels, the maximum of the narrow peak on the Green's function $G''_{mm}(\omega)$ of spin waves will touch the minimum of the dip on the Green's function of elastic waves $G''_{uu}(\omega)$ at any relations between $(\varepsilon/\varepsilon_0)^2$ and $(\Delta\varepsilon/\varepsilon_0)^2$ in both the standard and new SCAs. In [21], we suggested that this property is due to the uniform distribution of the energy between spin and elastic waves, which is satisfied only at the center of the gap at the point $k = k_r$, $\omega = \omega_r$:

$$G_{mm}(\omega_r, k_r) = G_{uu}(\omega_r, k_r). \qquad (67)$$

This suggestion is confirmed by the universality of law (67): it is valid both at any relations between $(\varepsilon/\varepsilon_0)^2$ and $(\Delta\varepsilon/\varepsilon_0)^2$and at any correlation wavenumbers of inhomogeneities k_c. Beyond the region of existence of resonance peaks in the fine structure of the spectrum, Eq. (66), which is obtained for the case $k_c = 0$, is approximately satisfied at nonzero k_c values.

We now consider the case of the correlation radius an order of magnitude smaller than that in Fig. 2. Figure 3 shows the imaginary parts $G''_{mm}(\omega)$ and $G''_{uu}(\omega)$ of the diagonal elements of the matrix Green's functions of spin and elastic waves, respectively, for the case $\kappa_c = 0.1$. It is seen that discrepancies between the results obtained in the standard and new SCAs decrease sharply with an increase in k_c. Dashed curves are now close to solid curves. Only signatures of the fine structure on the maxima of peaks hold (left panels of Figs. 3d and 3e). In this case, Eq. (67) remains valid. The results obtained in the standard and new SCAs coincide with each other at $k_c \gtrsim 0.5$. This corresponds to [14], where the Green's functions of waves in the inhomogeneous medium calculated in the standard and new SCAs coincided with each other at the same κ_c values.

We consider another situation that can appear at an increase in k_c. With an increase in $\Delta\varepsilon$ and with a decrease in ε at small k_c values, two narrow resonance peaks can be joined into one wide peak even at nonzero ε values (Fig. 4, red solid curve). We analyze the shape of the imaginary parts of diagonal elements of the matrix Green's function at fixed ratios $(\varepsilon/\varepsilon_0)^2 = 0.25$ and $(\Delta\varepsilon/\varepsilon_0)^2 = 0.75$ and at various κ_c values (Fig. 4). At small κ_c values, two peaks are already joined into one wide peak (red solid curve). The maximum of this peak in the spectrum exhibits a fine structure including a narrow peak (resonance) on the Green's function $G''_{mm}(\omega)$ of spin waves and a dip (antiresonance) on the Green's function $G''_{uu}(\omega)$ of elastic waves. With an increase in k_c at a fixed relation between $(\varepsilon/\varepsilon_0)^2$ and $(\Delta\varepsilon/\varepsilon_0)^2$, the fine structure at maxima of peaks disappears gradually and the single peak is again split into two peaks (black dashed line and blue dash-dotted curve). The width of each of these peaks decreases, whereas the height increases with a further increase in k_c. Similar to the single resonance studied in [14, 15], this effect is due to the partial averaging of inhomoge-

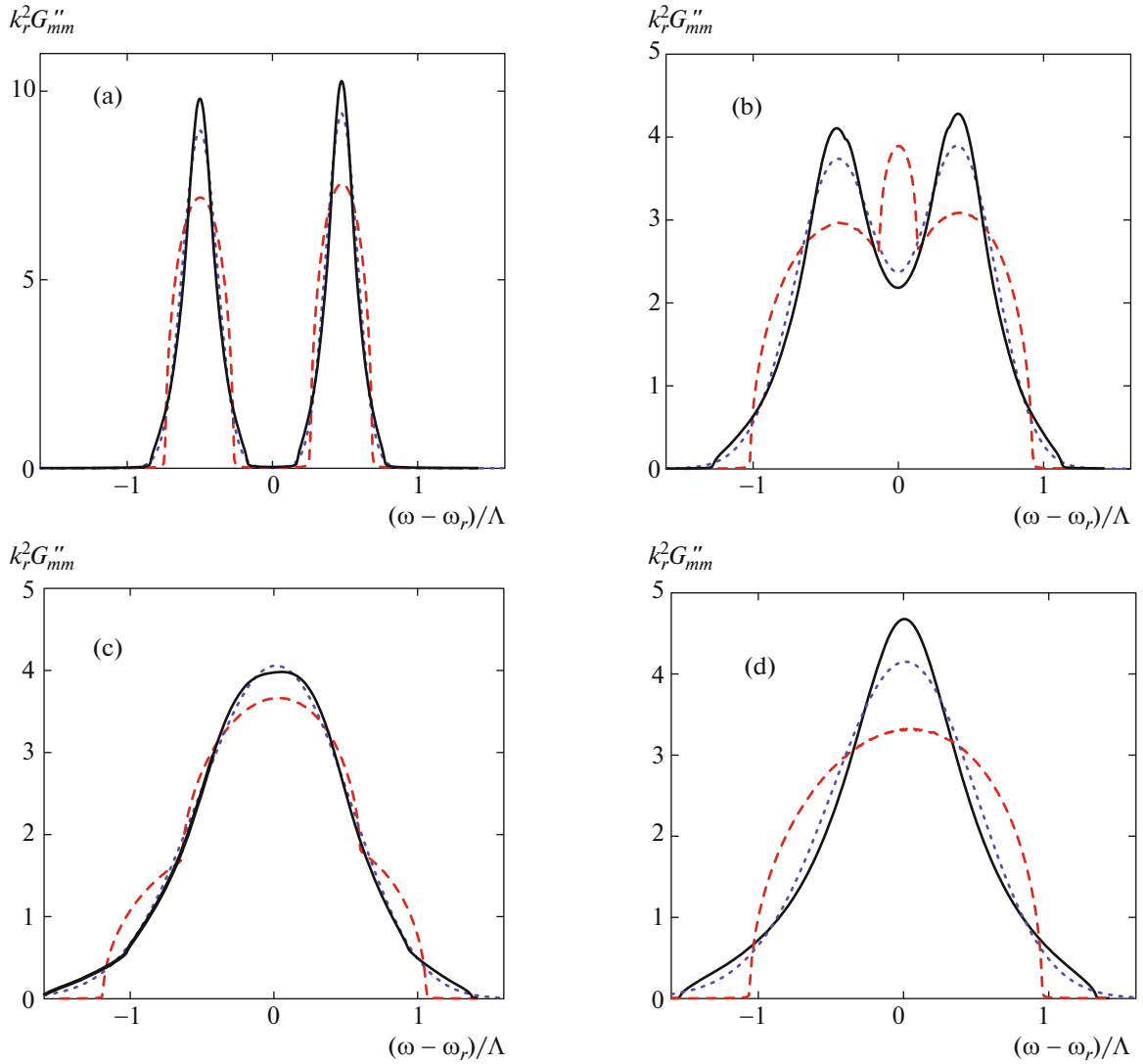

Fig. 1. (Color online) Imaginary parts $G''_{mm}(\omega)$ of the Green's functions of spin waves obtained (red dashed curves) in the standard SCA, (solid curves) in the new SCA, and (blue dotted curve) by the exact summation of all diagrams at $k_c = 0$, $(\varepsilon/\varepsilon_0)^2 =$ (a) 0.95, (b) 0.7, (c) 0.25, and (d) 0, and $(\Delta\varepsilon/\varepsilon_0)^2 =$ (a) 0.05, (b) 0.3, (c) 0.75, and (d) 1.

neities in the intervals corresponding to half the wavelength λ. Owing to this averaging, the shape of the matrix Green's function with an increase in k_c approaches the shape of magnetoelastic resonance in the effective homogeneous medium with the magnetoelastic parameter $\varepsilon < \varepsilon_0$. With an increase in $\Delta\varepsilon$ and a decrease in ε at a fixed k_c value, the peaks are again joined into one peak.

We now consider the off-diagonal elements G_{mu} and G_{um} of the matrix Green's function for the limiting case $k_c = 0$. To this end, it is sufficient to analyze one function G_{ij} related to G_{mu} and G_{um} as

$$G_{ij}(\omega) = \sqrt{\frac{\mu}{\alpha}} G_{mu}(\omega) = \sqrt{\frac{\alpha}{\mu}} G_{um}(\omega). \qquad (68)$$

The real, $G'_{ij}(\omega)$, and imaginary, $G''_{ij}(\omega)$, parts of the off-diagonal element are shown in Fig. 5 as calculated (red dashed lines) in the standard SCA, (black solid lines) in the new SCA, and (blued dotted lines) by exactly summing all diagrams by Eq. (64). Since the off-diagonal elements are proportional to ε, their amplitude decreases with an increase in $\Delta\varepsilon$ and vanishes at $(\Delta\varepsilon/\varepsilon_0)^2 = 1$ and $(\varepsilon/\varepsilon_0)^2 = 0$. This decrease in the amplitude corresponds to an increase in the scale of the ordinate axis in Fig. 5. It is seen that the shape of the Green's functions calculated in the standard SCA is quite strongly distorted as compared to the exact shape of these functions. At the same time, the shape of the Green's functions calculated in the new SCA is very close to the shape of exact Green's func-

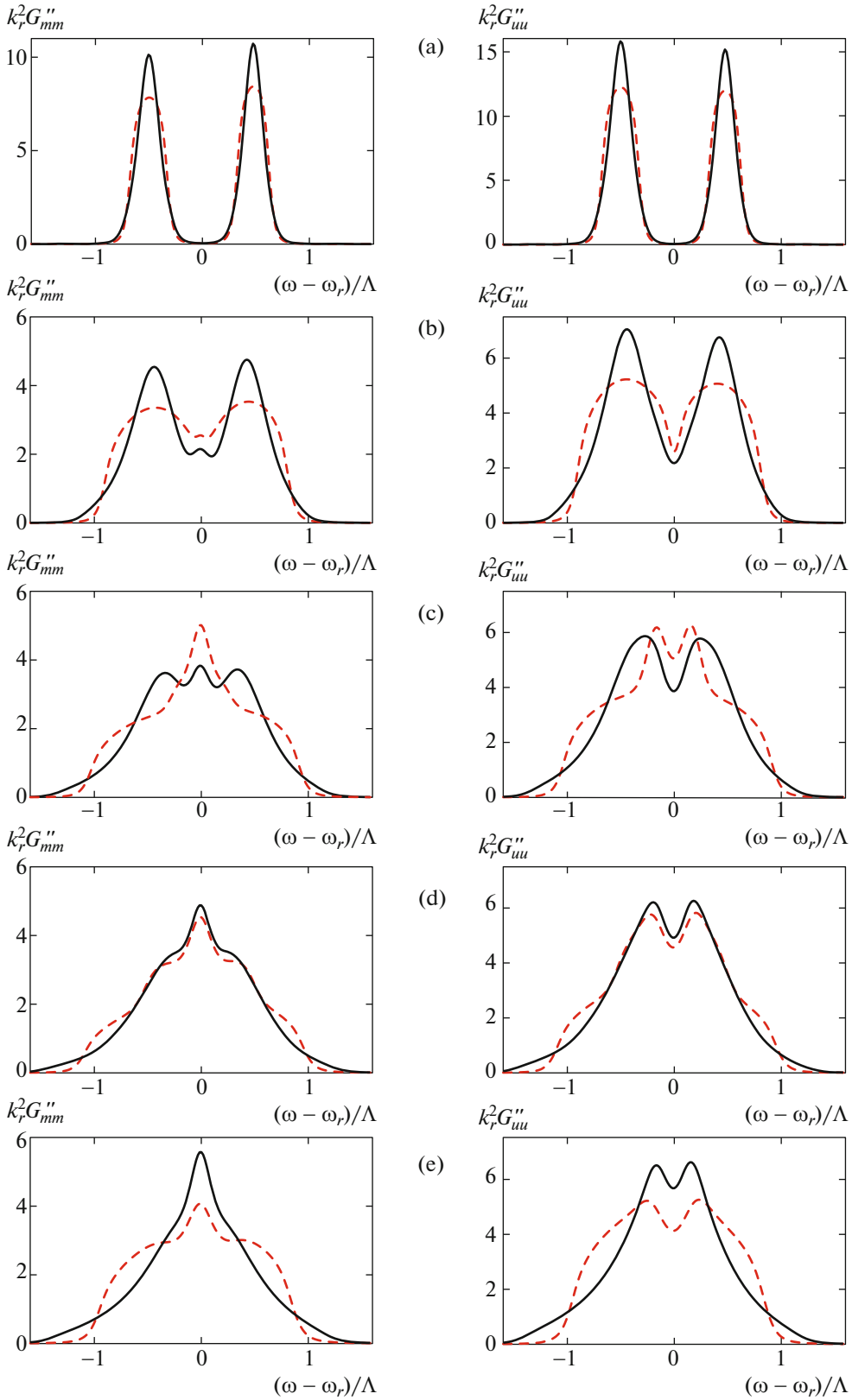

Fig. 2. (Color online) Imaginary parts $G''_{mm}(\omega)$ and $G''_{uu}(\omega)$ of the diagonal elements of the matrix Green's function of (left panels) spin and (right panels) elastic waves, respectively, in the (red dashed curves) standard SCA and (solid curves) new SCA at k_c = 0.01, $(\varepsilon/\varepsilon_0)^2$ = (a) 0.95, (b) 0.75, (c) 0.5, (d) 0.25, and (e) 0 and $(\Delta\varepsilon/\varepsilon_0)^2$ = (a) 0.05, (b) 0.25, (c) 0.5, (d) 0.75, and (e) 1.

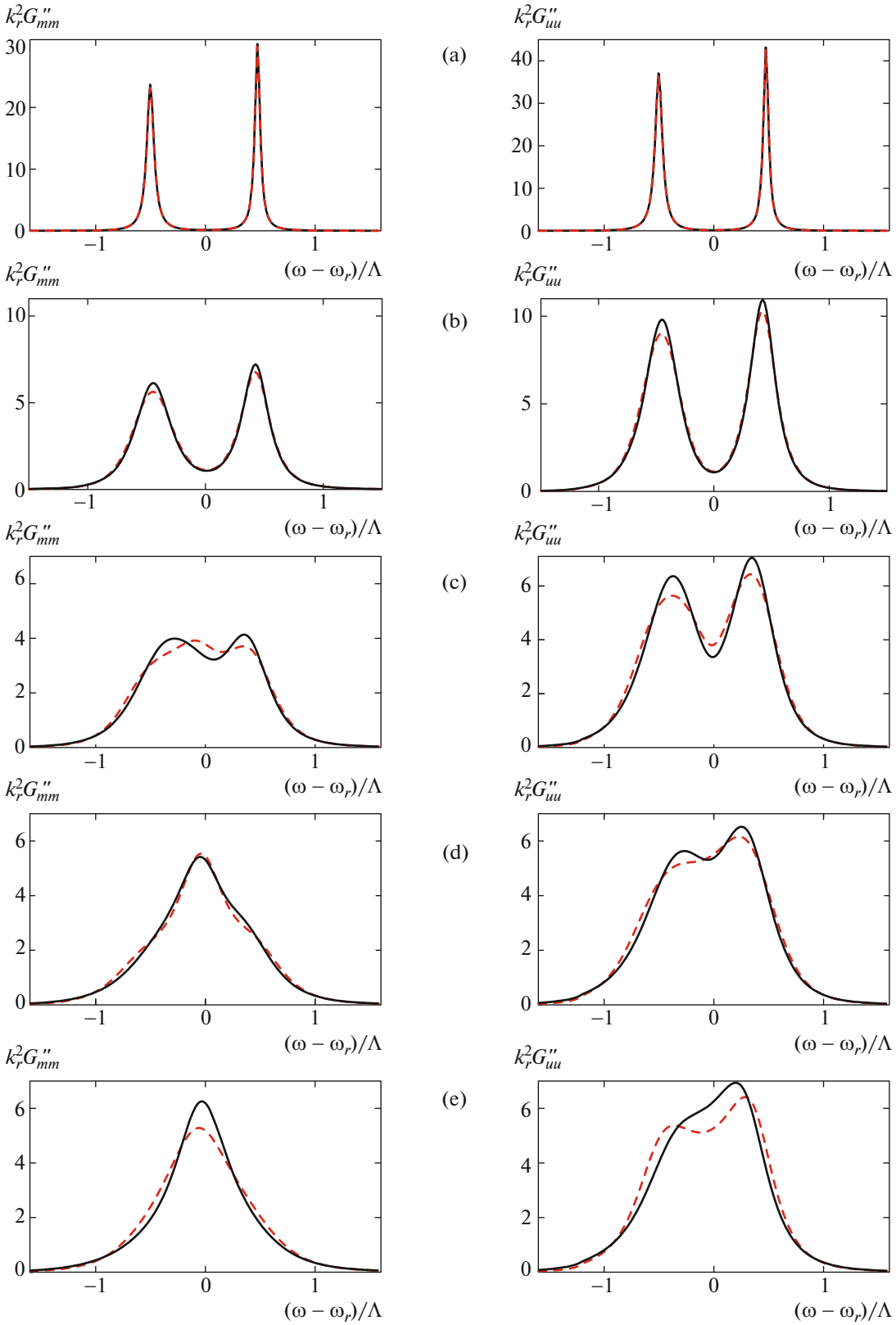

Fig. 3. (Color online) Imaginary parts $G''_{mm}(\omega)$ and $G''_{uu}(\omega)$ of the diagonal elements of the matrix Green's function of (left panels) spin and (right panels) elastic waves, respectively, in the (red dashed curves) standard SCA and (solid curves) new SCA at k_c = 0.1, $(\varepsilon/\varepsilon_0)^2$ = (a) 0.95, (b) 0.75, (c) 0.5, (d) 0.25, and (e) 0 and $(\Delta\varepsilon/\varepsilon_0)^2$ = (a) 0.05, (b) 0.25, (c) 0.5, (d) 0.75, and (e) 1.

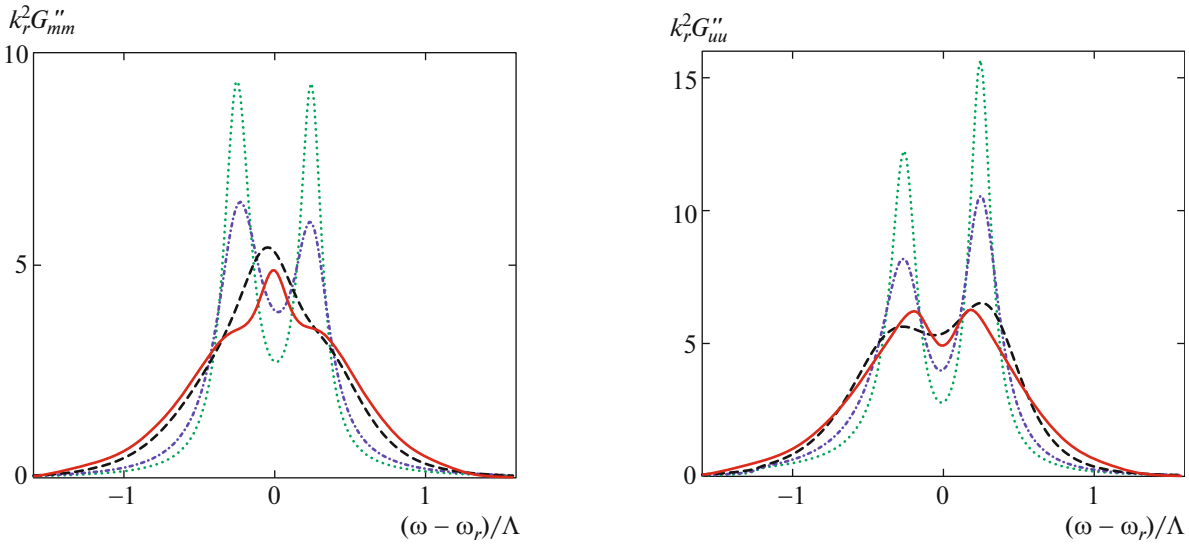

Fig. 4. (Color online) Imaginary parts $G''_{mm}(\omega)$ and $G''_{uu}(\omega)$ of the diagonal elements of the matrix Green's function of (left panel) spin and (right panel) elastic waves, respectively, in the new SCA at $(\varepsilon/\varepsilon_0)^2 = 0.25$, $(\Delta\varepsilon/\varepsilon_0)^2 = 0.75$, and k_c = (red solid curve) 0.01, (dashed curve) 0.1, (blue dash-dotted curve) 0.3, and (green dotted curve) 0.5.

tions. With an increase in nonzero k_c values, curves calculated in the standard and new SCAs approach each other and almost coincide with each other at $k_c \gtrsim 0.5$. It is noteworthy that the calculations in the new SCA confirm the absence of any fine structure in the spectrum of off-diagonal elements of Green's functions that was previously revealed in the standard SCA [22].

5. CONCLUSIONS

The aims of this work were (i) to generalize the new self-consistent approximation proposed in [14] to the system of two interacting wavefields and (ii) to develop a more accurate theory of magnetoelastic resonance in a inhomogeneous medium based on this generalization. The first aim is methodological. To achieve it, we have derived a system of self-consistent equations for the matrix Green's function and matrix vertex function including both the first and second terms of the expansion of the vertex function. The developed mathematical method can be used to analyze coupled oscillations of different physical nature in media with a partially or completely randomized coupling parameter such as polaritons and magnetoelastic waves. The method is applicable in a wide range of the correlation wavenumber k_c of inhomogeneities from $k_c = 0$ (infinite radius of correlations) to k_c values corresponding to the classical limit. However, it is reasonable to use this method in a much narrower range: the Green's functions calculated in the standard and new approximations approach each other with an increase in k_c and almost coincide with each other at $k_c/k \geq 0.5$. Therefore, for large k_c values, it is reasonable to use the simpler standard self-consistent approximation. It is remarkable that the same range of the correlation wavelength k_c of inhomogeneities where the standard and new approximations give different results was obtained for the problem of a single wavefield in the inhomogeneous medium [15]. In the limiting case of infinite radius of correlations ($k_c = 0$), in addition to approximate results, exact analytical expressions have been obtained by summing all diagrams of the elements of the matrix Green's function. In this case, we have compared the standard and new self-consistent approximations to exact analytical expressions. It has been shown that the new self-consistent approximation describes both the shape and width of resonance peaks corresponding to the exact plots of the Green's function.

We have applied the developed method to coupled magnetoelastic waves in a ferromagnet with an inhomogeneous magnetoelastic coupling parameter because the theory of magnetoelastic resonance in the inhomogeneous medium was developed in the standard self-consistent approximation in our previous works [20–23]. It was of interest to determine how the effects obtained within this theory change in the new self-consistent approximation. The main result provided by new method is the much better description of the shape of resonance peaks of the dynamic susceptibility. All effects obtained in the previous theory—the dome shape of peaks of magnetoelastic resonance, resonance curves with three maxima (independent of the fine structure resonance), and bends on the sides of resonance curves—appear to be due to disadvantage of the previous method. At the same time, the results describing the broadening and approach of magnetoelastic resonance peaks, as well as their joining into a

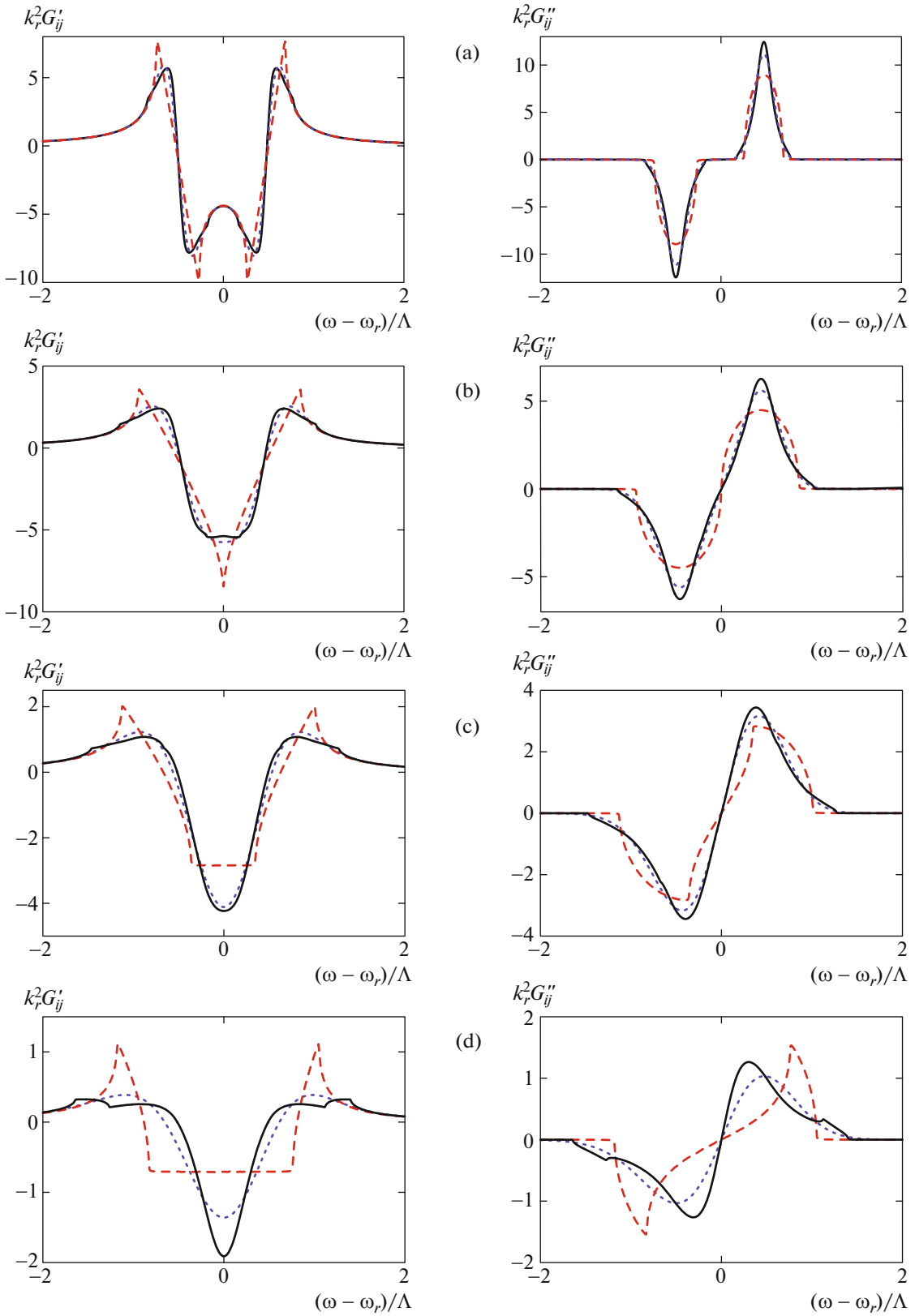

Fig. 5. (Color online) (Left panels) Real and (right panels) imaginary parts of the off-diagonal elements of the matrix Green's function obtained (red dashed curves) in the standard SCA, (solid curves) in the new SCA, and (blue dotted curve) by the exact summation of all diagrams at $k_c = 0$ and $(\varepsilon/\varepsilon_0)^2$ = (a) 0.95, (b) 0.8, (c) 0.5, and (d) 0.1, and $(\Delta\varepsilon/\varepsilon_0)^2$ = (a) 0.05, (b) 0.2, (c) 0.5, and (d) 0.9.

single wide peak with an increase in the rms fluctuation $\Delta\varepsilon$ and with a decrease in the average value ε of the coupling parameter, that were previously obtained in the standard self-consistent approximation hold qualitatively in the new theory, which only quantitatively corrects them. It is particularly important that the new theory confirms the fine structure of the spectrum including a narrow resonance peak on the Green's function of spin waves and a narrow dip on the Green's function of elastic waves. This effect has not yet been observed experimentally but should be manifested at the interaction between any wavefields of different physical nature. The magnitude of this effect is proportional to the ratio of the velocities of these fields at the crossing-resonance point. This ratio for magnetoelastic resonance is comparatively small and fine-structure peaks are low. However, there are interacting physical fields with a very large ratio of velocities (polaritons, electron–phonon interaction, etc.), for which fine-structure peaks can be high [27].

ACKNOWLEDGMENTS

This work was supported in part by the Complex Program II.2P (0356-2015-0411) of the Siberian Branch of the Russian Academy of Sciences.

REFERENCES

1. A. B. Migdal, Sov. Phys. JETP **7**, 996 (1958).
2. R. H. Kraichnan, J. Math. Phys. **2**, 124 (1961).
3. H. Bruus and K. Flensberg, *Introduction to Many-Body Quantum Theory in Condensed Matter Physics* (Ørsted Lab., Niels Bohr Inst., Copenhagen, Denmark, 2002).
4. J. Cai, X. L. Lei, and L. M. Xie, Phys. Rev. B **39**, 11618 (1989).
5. V. N. Kostur and B. Mitrovic, Phys. Rev. B **50**, 12774 (1994).
6. C. Grimaldi, L. Pietronero, and S. Strässler, Phys. Rev. Lett. **75**, 1158 (1995).
7. Y. Takada and T. Higuchi, Phys. Rev. B **52**, 12720 (1995).
8. O. V. Danylenko, O. V. Dolgov, and V. V. Losyakov, Phys. Lett. A **230**, 79 (1997).
9. G. A. Ummarino and R. S. Gonnelli, Phys. Rev. B **56**, R14279 (1997).
10. F. Cosenza, L. de Cesare, and M. Fusco Girard, Phys. Rev. B **59**, 3349 (1999).
11. O. V. Danylenko and O. V. Dolgov, Phys. Rev. B **63**, 094506 (2001).
12. J. P. Hague and N. d'Ambrumenil, J. Low Temp. Phys. **151**, 1149 (2008).
13. J. Bauer, J. E. Han, and O. Gunnarsson, Phys. Rev. B **84**, 184531 (2011).
14. V. A. Ignatchenko and D. S. Polukhin, J. Phys. A: Math. Theor. **49**, 095004 (2016).
15. V. A. Ignatchenko, D. S. Polukhin, and D. S. Tsikalov, J. Magn. Magn. Mater. **440**, 83 (2017); dx. doi. org/10.1016.j.jmmm.2016.12.058.
16. A. I. Akhiezer, in *Proceedings of the Conference on Physics of Magnetic Phenomena, Moscow, May 23–31, 1956* (Metallurgizdat, Sverdlovsk, 1956).
17. E. A. Turov and Yu. P. Irkhin, Fiz. Met. Metalloved. **3**, 15 (1956).
18. A. I. Akhiezer, V. G. Bar'yakhtar, and S. V. Peletminskii, Sov. Phys. JETP **8**, 157 (1958).
19. C. Kittel, Phys. Rev. **110**, 835 (1958).
20. V. A. Ignatchenko and D. S. Polukhin, Solid State Phenom. **190**, 51 (2012).
21. V. A. Ignatchenko and D. S. Polukhin, J. Exp. Theor. Phys. **116**, 206 (2013).
22. V. A. Ignatchenko and D. S. Polukhin, J. Exp. Theor. Phys. **117**, 846 (2013).
23. V. A. Ignatchenko and D. S. Polukhin, Solid State Phenom. **215**, 105 (2014).
24. R. C. Bourret, Nuovo Cim. **26**, 1 (1962).
25. S. M. Rytov, Yu. A. Kravtsov, and V. I. Tatarskii, *Introduction to Statistical Radiophysics, Pt. 2: Chaotic Fields* (Nauka, Moscow, 1978) [in Russian].
26. M. V. Sadovskii, *Diagrammatics, Lectures on Selected Problems on Condensed State Theory,* 2nd ed. (Inst. Elektrofiz. UrO RAN, Yekaterinburg, 2005; World Scientific, Singapore, 2006).
27. V.A. Ignatchenko, D.S. Polukhin, Phys. Proc. **86**, 117 (2017).

Translated by R. Tyapaev